Article

The Effects of Chemical Etching and Ultra-Fine Grain Structure of Titanium on MG-63 Cells Response

Denis Nazarov [1,2,*], Elena Zemtsova [1], Vladimir Smirnov [1], Ilya Mitrofanov [2], Maxim Maximov [2], Natalia Yudintceva [3] and Maxim Shevtsov [3,4]

1 Saint Petersburg State University, Universitetskaya Nab, 7/9, 199034 Saint Petersburg, Russia; ezimtsova@yandex.ru (E.Z.); vms11@yandex.ru (V.S.)
2 Peter the Great Saint Petersburg Polytechnic University, Polytechnicheskaya 29, 195221 Saint Petersburg, Russia; carlemeros@gmail.com (I.M.); maximspbstu@mail.ru (M.M.)
3 Institute of Cytology of the Russian Academy of Sciences (RAS), Tikhoretsky Ave. 4, 194064 Saint Petersburg, Russia; yudintceva@mail.ru (N.Y.); shevtsov-max@mail.ru (M.S.)
4 Radiation Immuno-Oncology Group, Center for Translational Cancer Research Technische Universität München (TranslaTUM), Klinikum Rechts der Isar, Einstein Str. 25, 81675 Munich, Germany
* Correspondence: dennazar1@yandex.ru; Tel.: +7-812-428-4033

Abstract: In this work, we study the influence of the surface properties of ultrafine grained (UFG) and coarse grained (CG) titanium on the morphology, viability, proliferation and differentiation of osteoblast-like MG-63 cells. Wet chemical etching in H_2SO_4/H_2O_2 and NH_4OH/H_2O_2 solutions was used for producing surfaces with varying morphology, topography, composition and wettability. The topography and morphology have been studied by scanning electron microscopy (SEM) and atomic force microscopy (AFM). The composition was determined by time of flight mass-spectrometry (TOF-SIMS) and X-ray photoelectron spectroscopy (XPS). The results showed that it is possible to obtain samples with different compositions, hydrophilicity, topography and nanoscale or/and microscale structures by changing the etching time and the type of etching solution. It was found that developed topography and morphology can improve spreading and proliferation rate of MG-63 cells. A significant advantage of the samples of the UFG series in comparison with CG in adhesion, proliferation at later stages of cultivation (7 days), higher alkaline phosphatase (ALP) activity and faster achievement of its maximum values was found. However, there is no clear benefit of the UFG series on osteopontin (OPN) expression. All studied samples showed no cytotoxicity towards MG-63 cells and promoted their osteogenic differentiation.

Keywords: titanium; ultrafine grained materials; chemical etching; surface science; osteoblast response

1. Introduction

Titanium and its alloys are the most suitable and widely used materials for producing orthopedic and dental implants [1–3]. Success of using these materials is caused by combination of unique mechanical properties and excellent biocompatibility [1,3]. The former are high strength, low density, and relatively low modulus of elasticity in comparison to other metallic biomaterials such as stainless steels and cobalt–chromium alloys [1,4]. The latter is due to presence of thin film (2–6 nm) of titanium oxide on the titanium surface. This film is biocompatible, chemically stable and provides strong biocorrosion resistance [3].

The alloys have much more suitable mechanical properties for medical application than pure titanium [5]. However, they are potentially more dangerous due to possible release of allergic, carcinogenic and toxic elements such as nickel, vanadium, niobium, aluminum etc. [4,6,7]. Therefore, pure titanium is still regarded as an indispensable material for the production of medical implants. To improve the mechanical properties of titanium, bulk nanostructuring of the material by the methods of severe plastic deformation (SPD) is

very effective [8–10]. The ultrafine-grained (UFG) titanium obtained by SPD has more than two-fold increased ultimate tensile and yield strength, fatigue strength, perfect fracture toughness and is closer to the required value of Young's modulus [8,11]. In addition, it was shown that UFG titanium can significantly improve adhesion, spreading, proliferation, differentiation, tissue mineralization in vitro and accelerate the osseointegration of the implant in vivo [12,13] in comparison with coarse grained (CG) titanium.

However, the improvement in the biomedical characteristics for UFG titanium is usually insufficient or not observed at all. UFG structuring changes mostly the structure and texture of the surface layer, and significantly less affects the composition, topography and morphology of the surface [12,13]. In this regard, additional methods are used to modify the relief, composition and morphology of the titanium surface to stimulate the bioactivity of the material. Among the surface modification methods, the most successful in practice is the SLA technology, which includes sandblasting followed by etching in a mixture of strong acids (HCl and H_2SO_4). SLA leads to formation of developed topography of surface which increases osseointegration rate [14]. Despite a number of advantages, this technology is rather complex and has a number of limitations. For example, to preserve the hydrophilicity of the surface of implants treated with SLA, they must be stored in saline solutions [15]. Moreover, sandblasting may not be effective for modifying the surface of porous implants. Liquid-phase chemical etching can be considered as an alternative to SLA. This method allows to form a developed relief and to adjust the composition of the implant surface by simple immersion in acid or base solutions [16–18]. One of the main advantages of this method is its simplicity and wide possibilities of regulating the resulting surface characteristics by varying the etchant type, its concentration, etching time and temperature.

Earlier we investigated in detail the etching features of UFG and CG titanium in H_2SO_4/H_2O_2 (sulphuric piranha—SP) and NH_4OH/H_2O_2 (ammonia piranha—AP) solutions. Namely, changes of topography and morphology of surface during etching were studied. Results showed, that it is possible to create different nanoscale, microscale and hierarchical nano-microscale structures on the titanium surface by varying composition of etchant and etching type. In this work we continue the study of chemical composition, wettability of the most promising etched UFG and CG samples and tested their biomedical properties in vitro using osteoblast-like (MG-63) cell line. Analysis of the results obtained can be very useful for determining the relationship between the physicochemical characteristics of the material and the cytological response.

2. Materials and Methods

2.1. Samples Preparation

UFG and CG titanium samples were prepared in Limited Liability Company "Nanomet", Ufa, Russia, from titanium Grade 4. Titanium rods of 1 m length were subjected to Equal-Channel Angular Pressing by ECAP-Conform processing at 400 °C. Five ECAP-Conform passes resulted in total accumulated true strain that was equal to 3.5. After processing, the billets drawing at 200 °C resulted in the production of UFG rods with a grain size about 200–300 nm [19,20].

Then the unprocessed CG (average grain size—25 mkm) and ECAP-processed UFG rods were treated by machining. Firstly, the rods were cut into discs (thickness of 2–3 mm) with the Buehler IsoMet 1000 (Buehler, Lake Bluff, IL, USA). Then, the discs were ground and polished by a semiautomatic Buehler MiniMet 1000 machine (Buehler, Lake Bluff, IL, USA) to mirror-like surface using 600, 800, and 1200 grit sandpapers and silicon dioxide nanoparticles suspension (20 nm). Prior to etching, the samples were cleaned repeatedly with acetone and deionized water in an ultrasonic bath for 15 min and dried in an Ar.

Finally, the samples were immersed into a Pyrex glass container with NH_4OH/H_2O_2 or H_2SO_4/H_2O_2 solutions at 20 °C. Temperature was maintained by thermostat Elmi TW-2.03. Piranha solutions were prepared from 50% *v/v* ammonium hydroxide (NH_4OH; Vecton, Saint-Petersburg, Russia), 36 N sulfuric acid (H_2SO_4; Vecton, Saint-Petersburg, Russia), and 30% aqueous hydrogen peroxide (H_2O_2; Vecton, Saint-Petersburg, Russia). The

volume ratio of reactants in both types of solutions was 7/3; etching times were 15 min and 2 h for NH_4OH/H_2O_2 and 15 min and 24 h for H_2SO_4/H_2O_2 solutions. Immediately after etching, the samples were taken out of the etchant and thoroughly washed in deionized water using an ultrasonic bath [19].

2.2. Samples Characterization

The topography of the samples surfaces was studied using a Solver P47 Pro (NT-MDT, Moscow, Russia) probe microscope in the tapping mode via atomic force microscopy (AFM). A total of five random positions on the sample surface were measured. The average mean value of surface roughness (R_a), root mean square roughness (RMS), and surface area difference (the percentage increase of 3D surface area over 2D surface area) were calculated by the associated Gwyddion 2.37 software. AFM surface parameters were calculated for every scan and the average values were obtained [19].

Untreated and treated samples were imagined with scanning electron microscope Zeiss Merlin operated at 15 kV. Microscope spatial resolution was around 1 nm and magnification up to 600,000. SE (secondary electrons) regimes were used. A total of four random positions on each sample surface were scanned.

Chemical composition of the samples surface was studied by X-ray photoelectron spectroscopy (XPS). X-ray photoelectron spectra were registered with a "Escalab 250Xi" (Thermo Fisher Scientific, Waltham, MA, USA). The samples were excited by Al Kα (1486.7 eV) X-rays for measurements. The spectra were automatically charge compensated by setting the binding energy of C 1s carbon line to 284.8 eV [21].

Wettability was evaluated by measuring the static contact angle (Biolin Scientific Theta Lite, Gothenburg, Sweden). Deionized water (5 μL) was dropped onto each specimen with an auto-pipette at 20 °C. The average contact angles were measured from 3 specimens of each group at 5–6 surface positions 10 s after the dropping [22].

Elemental depth profiling was also carried out with a time-of-flight secondary ion mass spectrometer (TOF SIMS 5 instrument, ION-TOF GmbH, Münster, Germany). Cs (0.5 keV, area 120×120 μm^2) and O_2 (0.5 keV, area 150×150 μm^2) were used for sputtering. The depth profiles were measured by dynamic SIMS mode using the primary ion gun (Bi$^+$ at an energy of 30 keV and a probe measured sample current of 3.1 pA, detection area 100×100 μm^2).

2.3. In Vitro Assessment of the Cellular Interactions

2.3.1. Cell Culture

Human osteosarcoma cell line MG-63 (ATCC® CRL-1427TM) were obtained from the Russian Cell Culture Collection at the Institute of Cytology of the Russian Academy of Sciences (RAS) (Saint Petersburg, Russia). MG-63 were harvested in CO_2-incubator (37 °C, 6% CO_2) in DMEM medium (Sigma-Aldrich, St. Louis, MO, USA) supplemented with 2 mM L-glutamine, 10% fetal bovine serum (FBS) and antibiotics (100 units/mL Penicillin G and 100 μg/mL Streptomycin).

2.3.2. Cell Morphology

MG-63cells were co-incubated on the surface of the samples for 24 h in a CO_2-incubator. After incubation, cells were washed with Dulbecco's Phosphate Buffer Saline (PBS) (Sigma-Aldrich, St. Louis, MO, USA) and fixed in 2.5% glutaraldehyde in 0.1 M cacodylate buffer (Sigma-Aldrich, St. Louis, MO, USA). Evaluation of the cells morphology was performed using SEM JSM-35.7 (JEOL, Tokyo, Japan).

2.3.3. Cell Viability and Proliferation

MG-63 cells were incubated with PBS (control sample) for 1, 6, 12, 24, and 48 h in a CO_2-incubator. After incubation, cells were washed and 0.4% Trypan blue exclusion test was used for assessment of viability. The 3-(4,5-dimethylthiazol-2-yl)-2,5 diphenyl tetrazolium bromide (MTT) assay was used to estimate the cytotoxicity of the samples.

Additionally, the Vybrant® MTT Cell Proliferation assay (Life Technologies, USA) was used according to the manufacturer's protocol. Cell proliferation was analyzed following 1, 6, 12 h, and 1, 2, 3, and 7 days of co-incubation on the samples.

2.3.4. Cells Osteogenic Differentiation Analysis

For evaluation of the cells osteogenic differentiation, we analyzed early marker alkaline phosphatase (ALP) and late marker osteopontin (OPN) [23]. The assessment was performed after 1 h, 1, 2, 7, 14, and 28 days of cells co-incubation on samples in a CO_2-incubator. According to the manufacturer's protocol we analyzed culture medium for the concentration of the proteins employing Alkaline Phosphatase Assay Kit (Colorimetric) (Abcam, Cambridge, UK) and Osteopontin N-Half ELISA Kit (Clon tech, Mountain View, CA, USA) [24].

3. Results

3.1. Morphology, Topography and Wettability

Based on our recent results [19] of the chemical etching features, we selected etched UFG and CG titanium samples with the maximal difference in surface morphology and topography. The SEM images of the samples are depicted in Figure 1. In general, the surface topography of UFG titanium is more developed (Table 1) and its nano and microstructures are more uniform. However, in general surface morphology of the etched CG and UFG samples coincides. Titanium etched in H_2SO_4/H_2O_2 during 15 min (SP-15) has no evident nano- or microstructures. Prolonged acid etching during 24 h (SP-24) leads to the formation of both microscale and nanoscale structures. However, the microscale relief of the UFG Ti is more developed. Samples etched in NH_4OH/H_2O_2 for 15 min (AP-15), unlike SP-15, have nanostructures on the surface. Nanostructures on the UFG-AP-15 completely cover the sample surface, but on the CG-AP-15, surface areas without nanostructures are visible. Microstructures on the both samples are almost hidden, with the exception of a small number of microscale pits. The 2-h AP-etched UFG and CG samples (AP-2) have nanoscale structures and microscale pits. The pits sizes are in the range of several micrometers, but the shape of the pits in sample CG-AP-2 is more elongated.
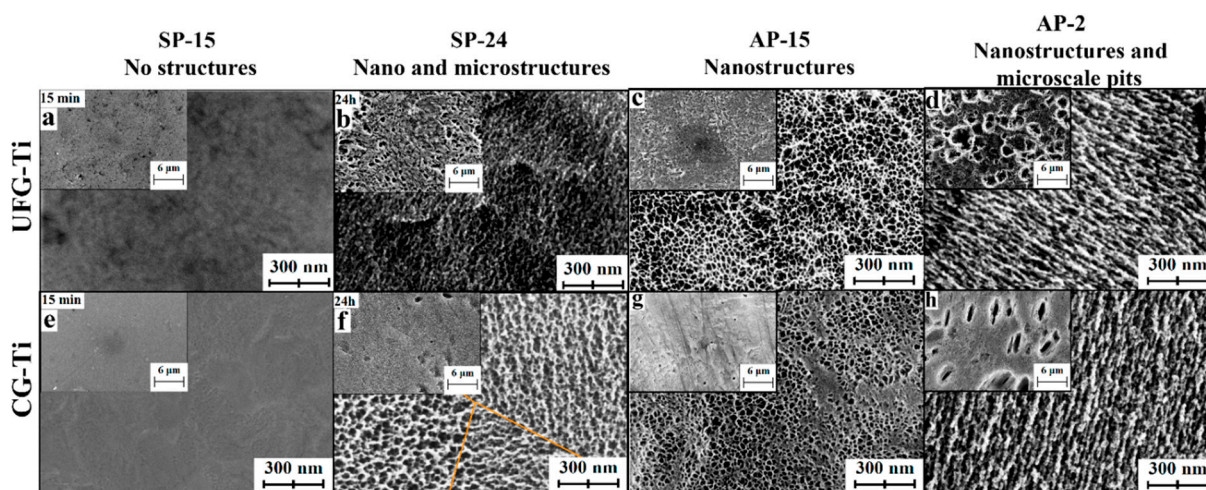
Figure 1. SEM images of chemically etched UFG and CG titanium discs: (**a**) UFG-SP-15; (**b**) UFG-SP-24; (**c**) UFG-AP-15; (**d**) UFG-AP-2; (**e**) CG-SP-15; (**f**) CG-SP-24; (**g**) CG-AP-15; (**h**) CG-AP-2. Reprinted with adaptation from [19].

The polished UFG and CG titanium surfaces (Table 1) are hydrophilic (wetting—79 ± 3° and 78 ± 4°) and have low roughness (RMS—6–7 nm) and surface area. The short etching in H_2SO_4/H_2O_2 (SP-15 samples) almost does not affect wettability and roughness. Prolonged etching in H_2SO_4/H_2O_2 (SP-24) slightly reduces the contact angles (from 79°

and 78° to 71° and 73° for UFG and CG, respectively), significantly increases the roughness and creates a developed surface topography.

Table 1. Wettability and surface topography parameters of the samples.

Sample	Wetting Angles °	Roughness [1] RMS, nm	[2] S_{surf}	Surface Characteristics
UFG-Ti	79 ± 3	6.54 ± 0.79	1.013 ± 0.003	Polished, native oxide, low roughness
CG-Ti	78 ± 4	6.33 ± 0.46	1.009 ± 0.001	
UFG-SP-15	75 ± 3	6.18 ± 0.76	1.010 ± 0.002	No micro/ nanostructures, low roughness
CG-SP-15	78 ± 2	6.13 ± 0.31	1.008 ± 0.001	
UFG-SP-24	71 ± 9	53.1 ± 6.5	1.065 ± 0.006	Nano and microstructures, high roughness
CG-SP-24	73 ± 7	28.4 ± 3.5	1.051 ± 0.005	
UFG-AP-15	101 ± 9	52.6 ± 5.2	1.151 ± 0.013	Nanostructures, high roughness
CG-AP-15	112 ± 14	23.9 ± 1.8	1.079 ± 0.005	
UFG-AP-2	120 ± 13	80.2 ± 5.2	1.350 ± 0.021	Nano and microstructures, high roughness
CG-AP-2	123 ± 17	95.1 ± 9.9	1.130 ± 0.016	

[1] RMS—Root mean squared roughness; [2] S_{surf}—surface area difference (the increase of 3D surface area over 2D surface area).

The etching in NH_4OH/H_2O_2 greatly increases the roughness and contact angles (101–123°) for both UFG and CG samples and they become hydrophobic (contact angles >90°). It should be noted that AP- etching results in a large scatter of contact angles due to high inhomogeneity of surface. The etched UFG samples have more developed topography and greater roughness. The contact angles of the UFG are less than the CG, but this difference is usually within the measurement error. In general, despite the difference in the topography of the UFG and CG series, their absolute values and the dispersion of contact angles almost do not depend on the titanium type, but are greatly determined by the chemical etching conditions.

3.2. Chemical Composition

The surface chemistry was not influenced by the changes in microstructure and texture induced by severe plastic deformation with ECAP [19,25]. Therefore we studied chemical composition by XPS and TOF-SIMS predominantly on the surface of polished and etched UFG titanium.

According to XPS survey spectra, titanium, oxygen, carbon and nitrogen were found on the surface of the samples. The sulfur from SP etchant was not detected in any of the samples [16]. High resolution N1s spectra (Figure 2a) showed that the most nitrogen was found on the surface of the AP-etched samples (2–3%). On the surface of the SP-etched samples, nitrogen content is much lower (<1%). Therefore, we assume that the nitrogen source is not only surface contamination, but also etchant residues and etching products for samples AP-15 and AP-2. Most of the nitrogen for AP-etched samples is probably originated from NH_4^+ (Figure 2a), but there are also N-C containing compounds.

In the C1s spectra (Figure 2b) for all samples single intensive peak at 284.8 eV corresponds to the aliphatic hydrocarbons (C-C, C-H) which are originated from surface contamination during storage the samples in air. Moreover, a small shoulder at higher binding energy (286.3 eV) assigned to C-OH. No additional peaks of oxygen-containing groups (aldehyde, carboxyl or carbonyl) in the range of 287–292 eV were observed.

The Ti2p spectra (Figure 2c) of polished and etched samples showed intensive Ti2p$_{3/2}$ and Ti2p$_{1/2}$ peaks at 458.7 and 464.4 eV (doublet gap is about 5.7 eV), which corresponded to TiO_2 [26]. An asymmetric peak at 453.4 eV for polished titanium and AP-etched titanium (inset Figure 2c) is assigned to metallic Ti [21]. This indicates that the surface oxide layer is very thin (no more than few nanometers). Upon etching in SP, this peak disappears, which indicates an increase in the oxide layer thickness due to surface oxidation. The deconvoluted Ti2p spectra (Figure S1) showed that the near-surface layer of the sam-

ples contains mainly TiO_2, but the non-etched sample and the AP-etched samples have significant amounts of TiO and Ti_2O_3 in addition to metallic titanium (Table 2).
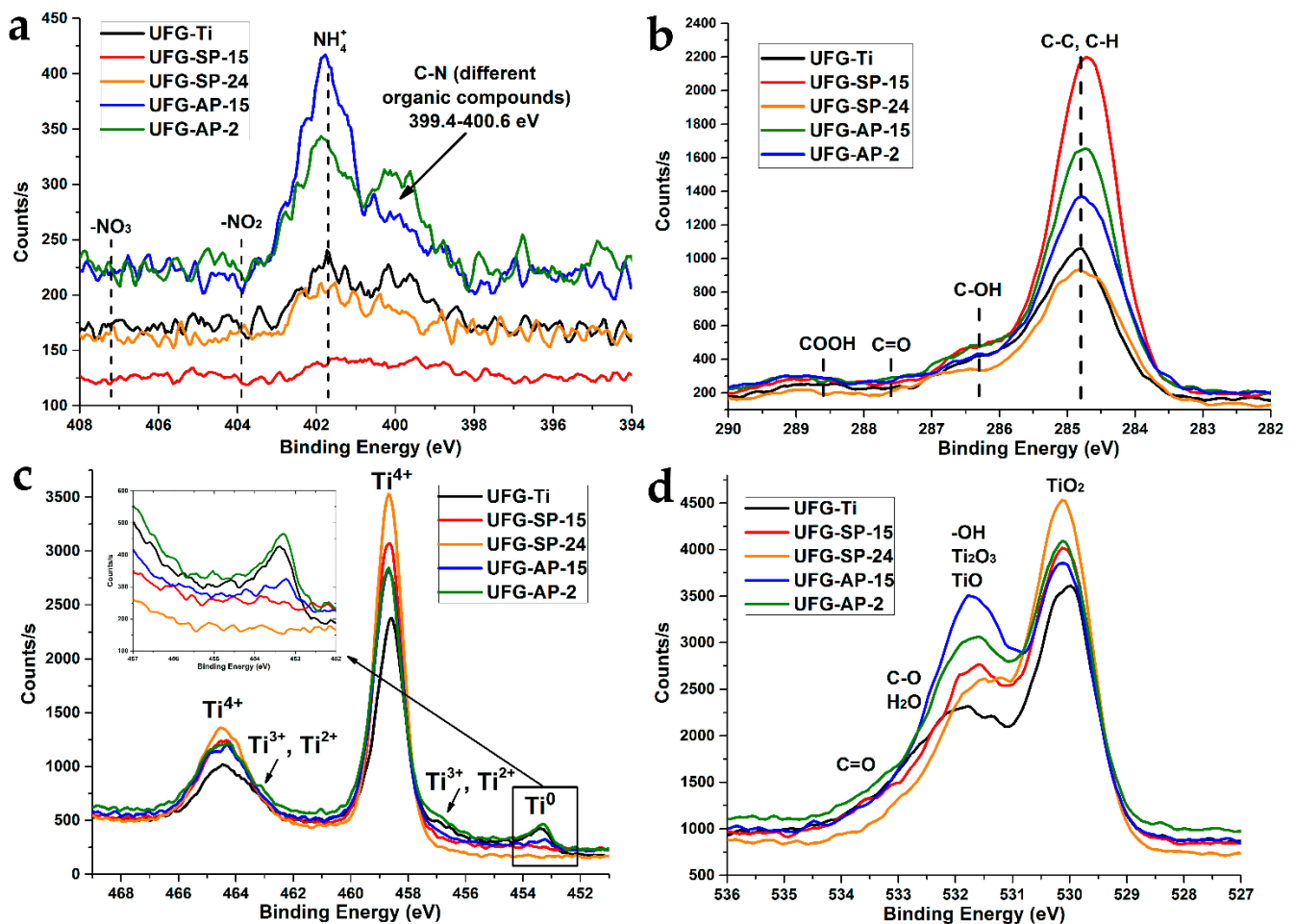

Figure 2. XPS spectra of polished and chemically etched UFG titanium: (**a**) N1s; (**b**) C1s; (**c**) Ti2p; (**d**) O1s.

**Table 2.** Percentage of Ti forms based on Ti2p spectra deconvolution.

Phase	UFG-Ti	SP-15	SP-24	AP-15	AP-2
TiO_2	73.2	90.0	91.7	83.7	77.9
Ti_2O_3	12.8	8.3	8.3	10.8	10.4
TiO	9.3	1.7	-	2.2	6.5
Ti	4.7	-	-	3.3	5.2

In the O1s spectra (Figure 2d), the peak at about 530.1 eV is assigned to TiO_2, and the peak at 531.7 eV can correspond to both hydroxyl—OH [27,28] and TiO/Ti_2O_3 [29], which are found in the Ti2p spectra. Moreover, a small shoulder in the region of 532–534 eV can be caused by the presence of the surface water [27,28] as well as organic contaminants (C-O, C=O) [30], which were also recognized in the C1s spectra. Deconvoluted spectra (Figure S2) showed that, for the UFG-Ti and SP-15 samples, the shoulder consists of at least two components ($C-O/H_2O$ and C=O). The AP-etched samples are characterized by a smaller TiO_2 amount and a higher amount of $OH/TiO/Ti_2O_3$ (Table 3). Unfortunately, it is rather difficult to deconvolute these components, because they are very close to each other and overlap a lot.

Table 3. Percentage of O forms based on O1s spectra deconvolution.

Phase	UFG-Ti	SP-15	SP-24	AP-15	AP-2
TiO_2	49.3	54.1	59.6	44.0	48.6
-OH, Ti_2O_3, TiO	30.3	31.1	29.2	42.3	35.5
C-O, H_2O	17.8	12.3	11.2	13.7	15.9
C=O	2.6	2.5	-	-	-

According to the TOF-SIMS results, polished and etched titanium surfaces contain both organic (CO^+, C^+, CH^-, C_2H^-, etc.) and inorganic (Fe^+, K^+, Cl^-, F^-) foreign ions (Figures 3 and S3). These ions disappear after ion sputtering of the surface layer and are probably caused by surface contamination during samples storage at ambient atmosphere. Sulfur-containing ions were not found, and only CN^- is clearly detected as nitrogen-containing ion.
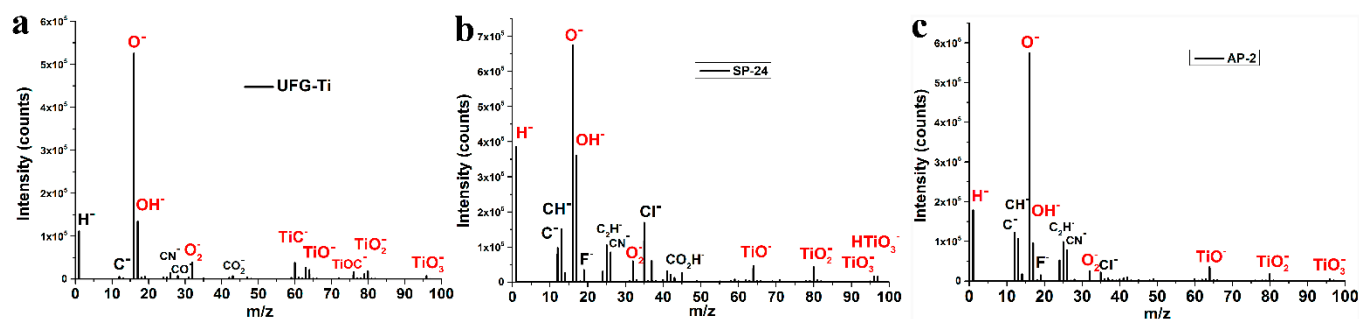
Figure 3. TOF-SIMS spectra of negative ions: (**a**) UFG-Ti; (**b**) UFG-SP-24; (**c**) UFG-AP-2.

The quantitative analysis of the TOF-SIMS spectra is difficult due to the difference in the nature and ionization degree of chemical groups of various types. Nevertheless, a comparison of the $O^-\backslash OH^-$ peaks intensities for different samples allows us to conclude that the content of hydroxyl groups on the surface increases upon 24 h SP-etching ($OH^-/O^- = 0.53$) and decrease upon 2 h AP-etching ($OH^-/O^- = 0.17$). The ratio OH^-/O^- for polished titanium was 0.26 (Figure 3).

Comparison of the $TiOH^+$ and $TiOOH^+$ ions intensities with respect to TiO^+ and TiO_2^+ (Figures S3 and S4) showed that, during SP-etching, OH^-/O^- ratio raised, and upon AP-etching, this ratio diminished. Thus, SP-etching increases the number of the surface hydroxide ions, while AP-etching decreases.

3.3. In Vitro Results

3.3.1. Spreading and Morphology of the Cells

After 24 h co-incubation of the MG-63 cells onto polished and etched UFG and CG titanium samples, they were washed with PBS and fixed for the subsequent SEM analysis (Figure 4). The cells incubated on CG titanium differ significantly from those incubated on UFG titanium. MG-63 cells cultured on the CG-SP-15 sample had a bipolar elongated shape, which most closely corresponded to the cell morphology on the surface of the polished CG-Ti sample and control (cultivation on plastic culture plate—Figure S5). On the surface of CG-SP-24 and CG-AP-15, along with the bipolar form, we detected strongly spread, rounded cells, as well as cells with long appendages. The peculiarities of cell cultivation on the CG-AP-2 sample include the ability of cells to form aggregates (Figure 4). The morphology of cells on the surface of the UFG samples has significant differences from the CG samples. The cells were elongated in shape, quickly formed a monolayer and form cell strands. Morphological differences between the samples were not revealed.
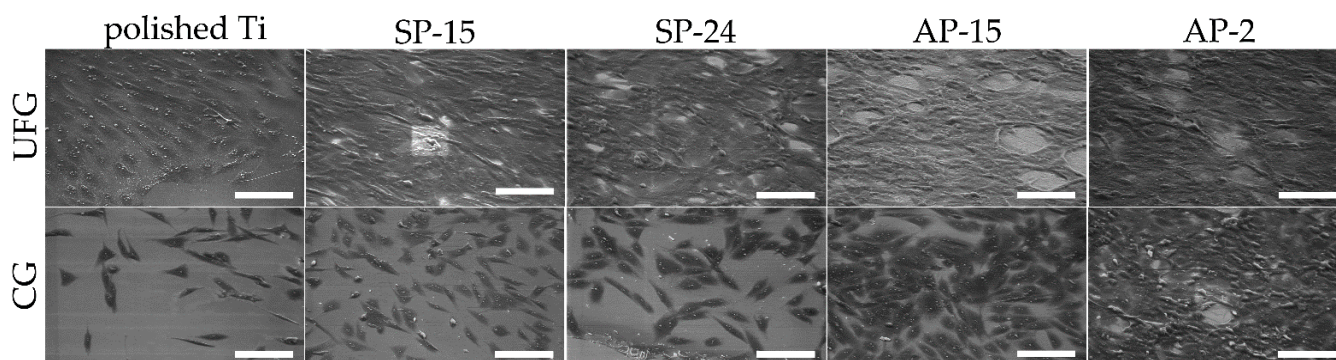
Figure 4. The morphology of MG-63 cells co-incubated after 24 h of cultivation. Scale bar—100 μm.

3.3.2. Cell Viability and Proliferation

We measured the cytotoxicity after 1, 6 and 12 h, 1 and 2 days co-incubation of the MG-63 cells employing MTT assay. MTT test shows the metabolic activity in cells and is influenced by proliferation rate. Therefore we used the short periods of cultivation to study viability of the cells. Results showed that all samples did not cause toxic activity for the whole 48 h period of observation (Figure 5). The difference between UFG and CG titanium (both polished and etched) was minimal. In the early stages (1 h) the CG series performed slightly better, but later (1–2 days) the UFG samples viabilities were higher. However, the results for all samples demonstrated no significant differences among the viability of the samples including control.
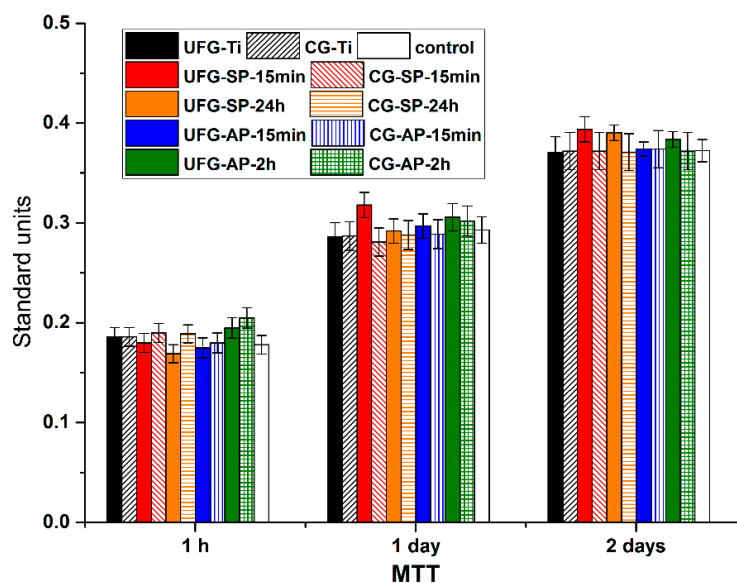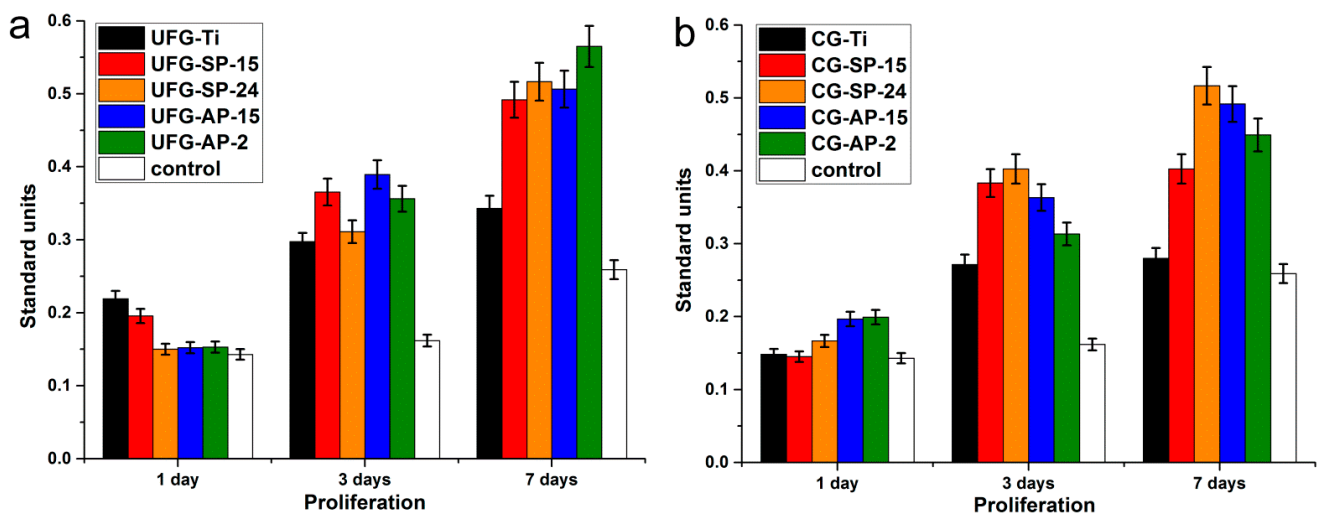

Figure 5. MG-63 cells viability after co-incubation on UFG and CG titanium. Data are presented as mean $\pm$ S.D. from five independent series of experiments ($p < 0.05$).

The proliferation of osteoblasts has been increased during the entire experiment (up to 7 days) (Figures 6 and S6). With an increase in the cultivation duration, the advantage of etched samples over non-etched ones gradually appeared and increased. Depending on the topography and surface morphology, the samples can be divided into 3 groups: the samples with smooth surface (UFG-Ti, CG-Ti, UFG-SP-15 and CG-SP-15), the samples with only nanostructures (UFG-AP-15 and CG-AP-15) and the samples with both micro- and nanostructures (UFG-AP-2, CG-AP-2, CG-SP-24, UFG-SP-24).

Figure 6. MG-63 cells proliferation activity after co-incubation on: (**a**) UFG samples; (**b**) CG samples. Data are presented as mean ± S.D. from five independent series of experiments ($p < 0.05$).

For samples with a smooth surface (black and red bars on Figure 6) the advantage of UFG samples (UFG-Ti, UFG-SP-15) over CG analogs and over UFG samples with a developed topography was noticeable at early cultivation stages (Figures 6 and S6). At later cultivation stages, the difference disappears. It should also be noted that etching in SP for 15 min accelerated proliferation at the later cultivation stages (3–7 days), despite the absence of a meaningful effect on the surface topography. It can be explained by the greater oxide layer thickness and an increase in the number of hydroxyl groups on the surface of SP-15 samples in comparison to untreated titanium.

For samples with nanostructures on the surface, there was a slight advantage of CG-AP-15 over UFG-AP-15 at early cultivation times, but it disappeared after 2–3 days (Figure S6, blue bars).

Samples of the SP-24 and AP-2 series (orange and green bars) had both nano- and microstructures. For SP-24 samples, there was a slight advantage of CG titanium over UFG, but it disappeared by 7 days. Probably, in this case, the more developed microscale topography of the UFG-SP-24 sample had a negative impact. There was also a difference for the AP-2 samples. The proliferation of the CG sample gradually increased, while for the UFG there is a very fast growth after 2 days (Figure S6). The narrow, long microscale pits of CG-AP-2 (Figure 1) are probably more favorable for rapid proliferation, however the rounded pits of UFG-AP-2 are better in the later cultivation stages.

Comparison of the proliferation results for the studied samples with the control showed that the difference is gradually increased with an increase in the cultivation time. The smallest difference between the samples and control was observed for untreated CG and UFG. Thus, chemical etching enhances MG-63 osteoblasts proliferation.

3.3.3. Cells Osteogenic Differentiation Analysis

Considering the ALP activity dynamics, one can notice a clear influence of the titanium type (CG or UFG), but the impact of surface morphology was not as great as in case of proliferation study (Figure 7). For all samples of etched UFG titanium, a clear maximum was observed around 7 days (Figure S7) and these values were significantly higher than those for similar CG titanium samples. ALP activity was gradually decreased for all etched UFG-samples since the 7th day of cultivation (Figure 7a). Polished UFG titanium had maximum of ALP activity at 14 days. The maximum ALP activity values in the entire investigated interval were noticed for UFG-SP-15, and its activity decreased more slowly than for other samples. For the CG series, no clear maximum was observed (Figures S7 and 7b). CG-Ti and CG-SP-24 are characterized by a slow decrease, while ALP activity of CG-SP-15 and CG-AP-2 was slowly increased. For the CG-AP-15, the values

were rather constant. It is possible that the maxima for the samples of the CG series should appear in the intermediate intervals (7–14 and 14–28 days).
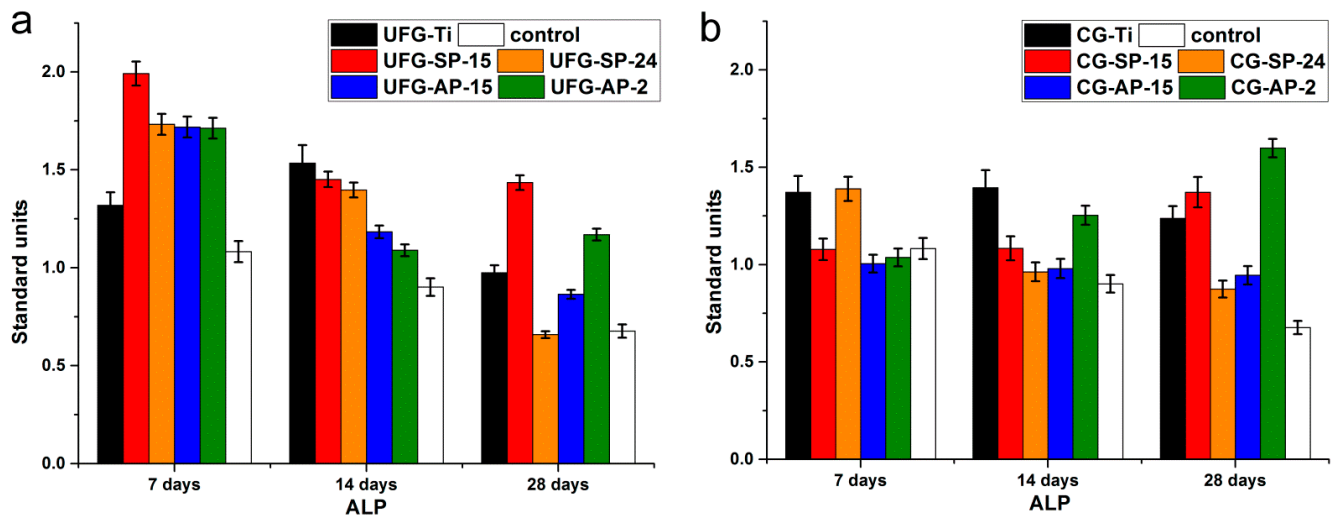
Figure 7. Alkaline phosphatase production by MC3T3-E1 osteoblasts on UFG series—(**a**) and CG series—(**b**). Each value represents mean ± S.D. from five independent experiments ($p < 0.05$).

The ALP activity dynamics in the control sample was not clearly expressed, the ALP activity values almost did not change (Figures 7 and S7), but the ALP activity values of the studied samples were generally higher than in the control. This may indicate the differentiation of MG-63 cells in the osteogenic direction for all studied samples.

The pattern of change in OPN expression demonstrated the difference between etched UFG and CG titanium, but it is not as pronounced as for ALP activity (Figures 8 and S8). For the UFG samples, a maximum was observed at 14 days, and the differences between the types of etching were insignificant. For CG samples, the maximum OPN expression for SP-24 and AP-2 is observed at 14 days, and for SP-15 and AP-15 at 7 days. However, it is likely that the real maximum for these samples was somewhere in the range of 7–14 days. A similar intermediate maxima are possible for the UFG samples.
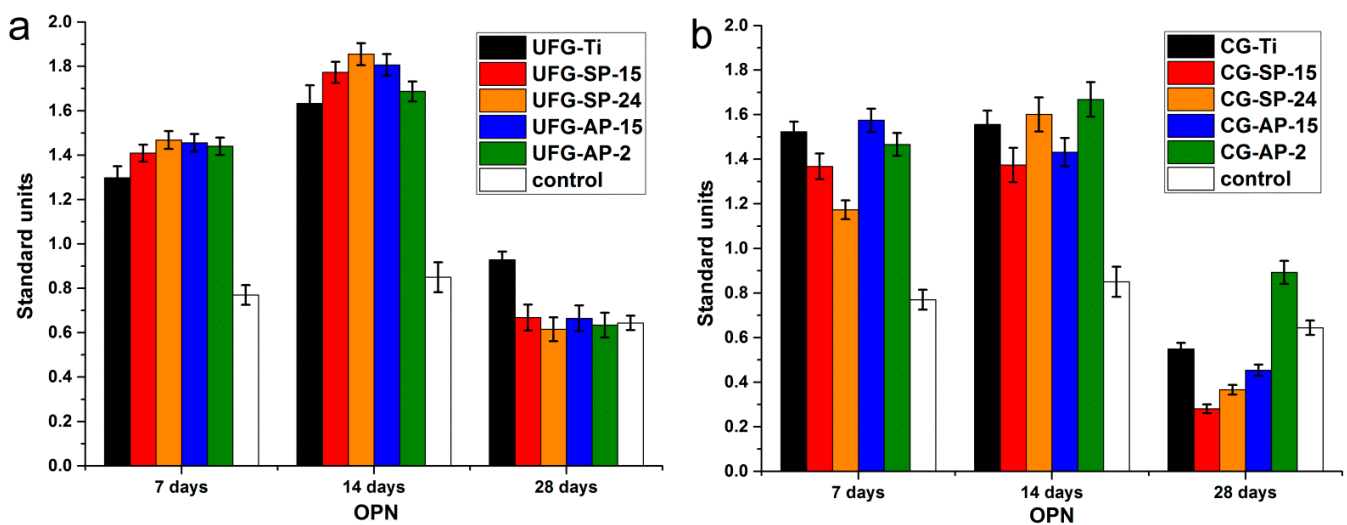
Figure 8. Osteopontin production by MC3T3-E1 osteoblasts on UFG series—(**a**) and CG series—(**b**). Each value represents mean ± S.D. from five independent experiments ($p < 0.05$).

The maximum absolute values of OPN expression were observed at 14 days of cultivation for UFG samples etched in H_2SO_4/H_2O_2 for 15 min and 24 h, as well as NH_4OH/H_2O_2 for 15 min.

Polished UFG and CG titanium showed maximum OPN expression at 14 days, and a significant difference between these samples is observed only at 2 and 28 days, when UFG-Ti shows significantly higher OPN expression than CG-Ti (Figure S8). The OPN expression dynamics of the control sample, in contrast to the studied samples, was not pronounced and the values changed insignificantly. Nevertheless, the absolute OPN expression values for the studied samples are much higher than in the control. It may indicate the stimulated differentiation of MG-63 cells in the osteogenic direction for all samples.

4. Discussion

The study of cell viability up to 2 days of cultivation times did not reveal any influence of either grain structure or etching conditions (Figure 5). Moreover, no significant difference was found between the studied samples and the control, i.e., cells cultured on the plastic plates. Therefore, all studied samples, regardless of the treatment conditions, are not cytotoxic to MG-63 cells.

On the other hand, the results obtained showed that the surface topography, morphology, wettability, composition, and grain structure of titanium affected significantly the morphology, proliferation, and differentiation of MG-63 cells. Unfortunately, it is rather difficult to distinguish the influence of individual factors, since they are closely related. For example, wettability depends on both the surface composition and the topography and morphology. The grain structure of titanium significantly affects the surface topography and morphology formed as a result of chemical etching [19]. In addition, it is rather difficult to change specific surface properties by chemical etching while maintaining other properties, since etching simultaneously changes both the topography, morphology, and surface composition.

Nevertheless, the results allow us to draw a number of conclusions. There are two main factors determining in vitro characteristics of our samples: the titanium grain structure and the surface morphology. Surface composition and wettability also appear to have a reasonable influence, but not the main and determining factor.

4.1. Affect of Grain Structure on Cell Morphology, Proliferation and Differentiation

Considering the differences in the in vitro characteristics of the CG and UFG series samples, the morphology of the cells is of particular interest. There is a large difference in morphology of MG-63 cells cultured on UFG and CG titanium (Figure 4). The cells on the etched UFG titanium have round shape, quickly form a monolayer and form cell strands, which indicates good and fast spreading and the potential for rapid proliferation and osteogenic differentiation. It is important to note that, for UFG series, no noticeable effect of the type and conditions of etching on cell morphology was found. Thus, the UFG structure of titanium is a sufficient condition for favorable adhesion and spreading of MG-63 osteoblast-like cells. In turn, the samples of the CG series had change in cell morphology which was observed under different etching conditions (Figure 4) and the CG structure is not sufficient for successful adhesion and rapid spreading of MG-63 cells.

In the study of cell proliferation, the difference between the control and studied samples is very clear (Figure 7). At the same time, there are also noticeable differences between similar samples of the UFG and CG series. At the maximum cultivation time (7 days), the advantage of most samples of the UFG series over CG ones is also significant. However, at shorter times, the difference was not observed, and the main proliferation determining factors were morphology, topography, and surface composition.

MG-63 osteoblast-like cell differentiation was studied using markers of early and late differentiation: ALP and OPN, respectively. ALP is a dephosphorylation catalyst that promotes the formation of crystallization centers of the inorganic component of bone tissue—hydroxyapatite [31]. OPN is a protein that plays an important role in bone

remodeling during osteosynthesis. So the OPN expression characteristics are indicators of the late osseointegration stages [31]. Considering an ALP activity and OPN expression, not only absolute values are important, but also their dynamics. In particular, reaching the maximum values of ALP and OPN and their subsequent decrease indicates the completion of certain stages of osteoblast differentiation.

Features of ALP activity and OPN expression changes of various samples indicate a significant effect of etching conditions on differentiation (Figures 7 and 8). However, the obtained data also reveals the difference between the UFG and CG series. For etched UFG samples, the maximum ALP activity was observed at 7 days, and the OPN expression was about 14. For the samples of the CG series, the dynamics of ALP and OPN was unclear. A clear maxima or change in the ALP activity and OPN production were not observed at the studied times and it were probably in the intermediate values of 7–14, 14–28 days. As in the case of studying the morphology of the cells, the dynamics of APL activity and OPN expression on the UFG samples were more similar to each other than on the CG samples.

To date, a large number of works have been published where the advantage of UFG titanium compared to CG analogues is shown based on in vitro tests using osteoblast-like cells (Table 4): In the study of Nie et al. [32] the preferential attachment, viability of MG-63 cells and promotion of ALP activity were showed. Zheng et al. [33] also revealed the enhanced cells adhesion and proliferation of MG-63 cells on UFG-Ti compared to CG-Ti. Much more research has been done using MC3T3-E1 preosteoblasts cells. A number of studies have demonstrated the advantage of UFG titanium in adhesion and spreading [34–36], viability and proliferation [34–38], and also ALP activity and OPN expression [35]. The positive effect of the UFG structure was found both for polished samples [32,34,37,38], and for samples with a rough surface that were obtained either by chemical etching in HCl and NaOH [33], SLA technology [36] or grit-blasting using hydroxyapatite particles [35]. However, it is worth noting that the above described positive effects of the UFG structure are often observed only at certain time intervals. For example Zheng et al. [33] showed the advantage of UFG titanium in adhesion only at the early stages (4 h) of MG-63 cells cultivation, and vice versa in proliferation at later ones (9 days). Zhao et al. [39] also noted no difference in proliferation of MC3T3-E1 cells after 7 days of cultivation and ALP activity after 14 and 21 days. The results of our study also showed a significant advantage of the UFG samples in comparison with CG ones in adhesion, proliferation at late stages of cultivation (7 days), higher ALP activity and faster achievement of its maximum values. However, in terms of OPN expression, the superiority of the UFG series samples cannot be asserted with certainty.

Table 4. Affect an UFG structure on in vitro cellular response.

Treatment	CG-Ti/UFG-Ti Grain Size, μm Roughness, nm Wettability, °	Cell Type	In Vitro Results: Advantage of UFG Over CG Titanium	Ref
ECAP Annealing polishing	-/0.28 120 ± 33/56.9 ± 9. 66.2 ± 4.0/57.9 ± 2.4	human osteoblast-like MG-63	No difference in the cell attachment and proliferation on CG and UFG samples up to 7 days in culture. Similar ALP activities on UFG and CG after 14 and 21 days	[39]
ECAP polishing	-/0.25 -/- -/-	osteoblast cell lines MG-63	Preferential attachment and viability The ALP activity was promoted on UFG samples	[32]
ECAP Etching in HCl Immersion in NaOH	-/0.28hierarchical porous surface	osteoblast-like MG-63	Enhanced cells adhesion (4 h) and proliferation (9 days) both for smooth and surface modified UFG. No affect in adhesion at 24 h and proliferation at 3 and 7 days	[33]

Table 4. *Cont.*

Treatment	CG-Ti/UFG-Ti Grain Size, μm Roughness, nm Wettability, °	Cell Type	In Vitro Results: Advantage of UFG Over CG Titanium	Ref
ECAP Polishing	4.5/0.2 -/- -/-	MC3T3-E1	Enhancement of cell proliferation and viability after 7 and 12 days in culture	[37]
C-ECAP Polishing	10.9/0.24 RMS before/after polishing: CG—40.2/0.24 nm UFG—70.2/0.3 nm	MC3T3-E1 pre-osteoblastic cells	The proliferation of cells on polished UFG-Ti exceeded unpolished CG-Ti 3.04-fold after 72 h	[38]
HPT (high pressure torsion) polishing	-/0.01−0.05 $1.9 \pm 0.8/1.2 \pm 0.4$ $69.9 \pm 5.4/62.0 \pm 3.9$	MC3T3 mouse pre-osteoblast	Improved cell adhesion and growth rate. Higher density of cells on the surface of nanograined samples	[34]
ECAP	40/0.4 -/- -/-	MC3T3 pre-osteoblast cells	The number of attached cells was higher on the samples having more (0002) plane parallel to the surface regardless of their grain sizes	[40]
HPT [1] HF etching	$118 \pm 49/0.1$ $190 \pm 10/279 \pm 20$ 51/40	MC3T3-E1 osteoblast cells	UFG Ti exhibited better cell adhesion and proliferation after etching than those of the CG. Cells on the rough surface spread well and developed their fibers widely as a dendritic shape	[41]
ECAP grit-blasting using HA [2] particles	-/0.2–0.3 $1980 \pm 290/1910 \pm 250$ $52.5 \pm 2.0/45.8 \pm 1.6$	MC3T3-E1 cells	Enhanced cell spreading, attachment, viability. Notably higher ALP and OPN levels in cells	[35]
ECAP SLA	-/0.2–0.3 $3.62 \pm 0.27/3.85 \pm 0.13$ $106.0 \pm 2.9/65.4 \pm 2.0$	MC3T3-E1 cells from mouse calvaria	The adhesion, proliferation and viability of cells cultured on the UFG-Ti were superior to that of CG-Ti	[36]

[1] HPT—high pressure torsion; [2] HA—hydroxyapatite.

Despite the large number of studies, the mechanism of the UFG structure influence on the biomedical properties of titanium is not completely clear. According to most studies, the original polished coarse-grained titanium is hydrophilic. Average values of contact angles for polished CG titanium range within 66.2–74.6° [34,39,42–47]. Contact angles of UFG Ti obtained by the ECAP is in all cases a few degrees less than CG-Ti and varies within 69.7–56.2° [39,42,43,45,46]. The CG and UFG titanium used in our study had contact angles of $79 \pm 3°$ and $78 \pm 4°$ respectively (Table 1). These values were higher than in the most studies. The contact angles of etched samples of the UFG series are slightly lower than for similar CG samples, but the difference is very small. Thus, it is unlikely that the surface wettability would affect the difference in in vitro results for UFG and CG samples in our study. The chemical composition of the surface is also independent on the grain structure, but is determined by the etching conditions [19]. Thus, significant factors determining the difference in the morphology and differentiation of MG-63 cells between the CG and UFG series should be either the grain structure (grain size, structure, size and density of grain boundaries), or the features of surface morphology and topography. In our previous study [19] it was shown that micro- and nanostructures obtained by etching UFG titanium were more uniform and had a more developed surface topography (Table 1) than CG samples. In addition, depending on the grain structure of titanium, some shape features of the resulting structures (Figure 1, samples AP-2) appeared. However, these differences were not as large as the differences achieved by changing the etching conditions. At the same time, the differences in in vitro properties for the CG and UFG series are much greater than for samples of the same series, but treated in different etching conditions. Therefore,

these differences of surface properties arising from etching of UFG and CG titanium can hardly determine the difference in in vitro characteristics of these two series. In addition, in vitro differences were found for the polished UFG and CG titanium samples, which had very similar morphology and surface topography.

A more likely reason for the difference in the behavior of osteoblast-like cells may be the difference in the number and density of intergranular boundaries of UFG and CG titanium. So recently Lowe et al. [38] found that cell proliferation correlate with the average grain boundary length per surface-attached osteoblasts MC3T3-E1. In addition, the surface texture can have a great influence on the cellular response. For example Hoseini et al. found that the number of attached MC3T3 pre-osteoblast cells is higher on the samples having more (0002) plane parallel to the surface regardless of their grain sizes [40]. It was assumed that enhancing the cell substrate interactions arises due to an increase in the number of hydroxyl groups, which are more densely packed on basal planes of surface. It was concluded that the texture plays a more important role than the grain size in the biocompatibility of pure titanium, but the SPD technology that produces UFG Ti has a significant effect on texture [48]. Surface energy can be an important factor determining the adhesion of osteoblasts. Bindu et al. showed in vitro and in vivo that surface stresses and defects of UFG Ti affect wettability and surface energy, which increases fibronectin adsorption and enhances 3T3 fibroblasts attachment [45].

Although most researchers agree that UFG titanium is much better than CG counterpart (Table 3), the advantage is not always observed and is often small. The results of our study do not give an unambiguous answer, but we can confidently state that the use of UFG titanium opens up new opportunities for creating new successful biomaterials in combination with other methods of material modification.

4.2. Affect of Etching Conditions on In Vitro Results

Now a large number of works are based on studies the effect of chemical etching of titanium in NH_4OH/H_2O_2 and H_2SO_4/H_2O_2 on the adhesion, proliferation and differentiation of osteoblasts-like cells (Table 5). It should be noted that the physicochemical characteristics of the surface obtained in our work agree with the results of other researchers. Etching in NH_4OH/H_2O_2 leads to the formation of micron/submicron structures [49] and a hydrophobic surface during storage of samples in air [50]. Etching in H_2SO_4/H_2O_2 leads to surface oxidation, an increase in the oxide layer thickness [16] and the formation of a hydrophilic network of nanopores and nanopits [16,51–53].

Nevertheless, despite the similarity of the physicochemical properties of the samples, there is a significant difference in the results of in vitro studies by various researchers. It was shown in [16] that etching in NH_4OH/H_2O_2 did not affect adhesion, but at the same time has a negative effect on the viability and proliferation of MC3T3-E1 osteoblasts, and also reduces mineralization after 14 days of cultivation. Deterioration of adhesion, proliferation, and differentiation of MC3T3-E1 cell also was shown by us previously for UFG titanium samples etched both in NH_4OH/H_2O_2 and H_2SO_4/H_2O_2 [22]. On the other hand, Yuan et al. [54] showed that etching in NH_4OH/H_2O_2 has a small but still positive effect on MG63 preosteoblasts attachment, proliferation and osteogenic differentiation (Table 5). The beneficial effects of NH_4OH/H_2O_2 treatment on MG63 cells attachment area, proliferation rate, ALP activity and OPN production were also showed by Zhang et al. [49]. The results of in vitro studies of samples etched in H_2SO_4/H_2O_2 [16,52,53,55–57] were more unambiguous and show that such treatment significantly improves the adhesion, proliferation and differentiation of MG-63 and MC3T3 pre-osteoblasts.

Table 5. Affect piranha etching on in vitro cellular response.

Treatment	Surface Characteristics	In Vitro Results	Ref
E-ultrasonically etching in NH_4OH/H_2O_2 for 2 h at 45 °C SE—SLA [1] + E	Hierarchical structures with micro holes of 10–30 μm in diameter and nano pits of tens nanometers in diameter on E and SE	Boost of osteoblasts MG63 attachment, proliferation and osteogenic differentiation on E and especially on SE.	[54]
NH_4OH/H_2O_2 (1:3, *v/v*)—E (plates), EB (bricks) NH_4OH/H_2O_2 + HCl/H_2SO_4—DE	E, DE: holes of 10–20 μm E, DE, EB are hydrophobic, EB stayed hydrophilic after 5 days' exposure to air.	Human osteoblast-like MG63 cells cultured on E and EB showed higher proliferation rate and attachment area than on DE and P. E and DE showed higher ALP activity after 7 and 14 days, while EB showed the highest OPN production after 21 days.	[49]
NH_4OH/H_2O_2 (50%/30%) H_2SO_4/H_2O_2 (36N/30%)	AP- pits diameter 50–100 nm, raising the percentage of peroxide resulted in an increase of the pit diameter, SP—spongelike network of nanopores	NH_4OH/H_2O_2—No impact on adhesion, but decrease the number of osteoblasts MC3T3-E1. H_2SO_4/H_2O_2 improve adhesion and spreading, accelerating proliferation and differentiation	[16]
NH_4OH/H_2O_2 (50%/30%) H_2SO_4/H_2O_2 (36N/30%) *v/v* ratios—7/3	microstructures, nanostructures, and hierarchical micro-/nanostructures	Deterioration of adhesion, proliferation, and differentiation of MC3T3-E1 osteoblasts cell for etched samples as compared to the non-treated ones	[22]
ECAP H_2SO_4/H_2O_2 3:1 *v/v* 2 h	Nanopits, sponge-like structure, sharp groves distributed uniformly with high surface roughness Contact angle before etching—58.8°, After—43.2°	adhesion and proliferation of hFOB [3] cells on ECAP and etched ECAP samples was found to be superior to that of control unprocessed sample. the formation of apatite on the piranha treated samples containing OH^- was improved	[55]
H_2SO_4/H_2O_2 3:1 ratio, 2 h	evenly distributed nanopit like structures, wettability after etching ~60°	Human osteosarcoma cell lines MG-63 cultivated on piranha treated Ti showed higher viability	[53]
10N H_2SO_4 and 30% H_2O_2 (1:1 *v/v*) for 4 h at RT [4] under agitation	network of nanopores	[2] BMP-9 increased pre-osteoblastic MC3T3-E1 differentiation irrespective of Ti surface topography; however, the cells grown on Ti-Nano were more responsible to BMP-9	[52]
10N H_2SO_4 and 30% H_2O_2 (1:1 *v/v*) at RT [4] under agitation, 4 h	nanotopography	nanotopography induces osteoblast MC3T3-E1 differentiation	[56]
concentrated H_2SO_4 (98% mass fraction) and 30% H_2O_2 (1:1 *v/v*) at RT [4] 1.5 h	Nanotopography mono-planar nanoporous surface with a pore diameter of 20 ± 5 nm	Increases in the adhesion formation per MC3T3-E1 cell area, focal adhesion length, and maturity on the nanoporous surface. Gene expression for various focal adhesion markers was significantly increased. More filopodia on cells grown on the nanoporous surface	[57]
50:50 mixture of 96% H_2SO_4 and 30% aqueous H_2O_2 (cooling bath) (10 mL/disc) and kept for 1.5 h under agitation	Hydrophilic after etching Hydrophobic after aging Aging for 4 month leads to crystallization	No difference in mouse calvaria-derived MC3T3 osteoblasts adhesion, spreading and growth on amorphous and crystalline surfaces. The number of focal adhesions was similar, cells on the amorphous surface exhibited a higher frequency of mature adhesions	[58]

[1] SLA—Sandblasting and acid-etching; [2] BMPs—bone morphogenetic proteins; [3] human fetal osteoblast; [4] RT—room temperature.

Of particular interest is the work [55], in which an adhesion and viability/proliferation of human fetal osteoblast (hFOB) cells were studied on polished and etched in H_2SO_4/H_2O_2 UFG titanium. The authors demonstrated a positive effect of the combination of UFG structure and etching, but that only etching had a significantly smaller effect on adhesion and proliferation than combination of etching and UFG structuring. The results of our study also showed that the grain structure of titanium significantly influenced the morphology and differentiation of osteoblast-like cells, but the conditions of chemical etching turned out to be an equally important factor influencing proliferation and differentiation.

As mentioned above, no any effect of etching conditions was found on the cell morphology for the UFG series; however, for CG titanium, this effect is clearly noticeable. Samples without developed topography (CG-Ti and CG-SP-15) showed low spreading, while samples with nanostructures (CG-AP-15) and hybrid nano/microstructures (CG-SP-24) strongly spread and had rounded cells with long appendages (Figure 5). The CG-AP-2, which has the developed nanotopography and microscale pits, showed the best spreading and ability to form aggregates of cells. Thus, morphology and surface topography determined the morphology and spreading of MG-63 cells for CG samples. Many reports indicate that osteogenic cells tend to attach and migrate significantly better onto hydrophilic surfaces rather than hydrophobic material due to high surface energy [3,41,59]. Although there are a number of works showing that the difference is either absent or minimal. For example Contreras et al. found no difference in spreading and adhesion of osteoblasts MC3T3 on the surface of samples with the same morphology, but different wettability and crystal structure [58]. It is noteworthy that in our study, hydrophilic samples (CG-Ti, CG-SP-15, CG-SP-24) showed even worse cell morphology than hydrophobic ones (CG-AP-2 and CG-AP-15). Therefore, we can assume a minimal effect of the wettability on the morphology of MG-63 cells, but the morphology and surface topography play the main role.

The proliferation of MG-63 cells is significantly increased for etched samples as compared to non-etched ones, which is especially noticeable at maximum study times (Figure 7). It is also clearly noticeable that the more developed the relief and morphology, the faster proliferation rate. However, it is worth noting a considerable difference between the samples of polished titanium (UFG-Ti, CG-Ti) and etched in H_2SO_4/H_2O_2 for 15 min (UFG-SP-15, CG-SP-15). Despite the absence of any structures and the flat surface of these samples, the latter show much more proliferative activity than the former. The difference is obviously due to the greater thickness of the oxide layer and the number of hydroxyl groups on the etched surface. Thus, surface morphology and topography play a decisive role in the proliferation of MG-63 cells, but the surface composition and grain structure of titanium (see Section 4.1.) also significantly affect proliferation.

The nature of osteogenic differentiation, as shown above, is significantly influenced by the grain structure of titanium. The effect of chemical etching is also clearly noticeable, however, it is impossible to conclude unambiguously about the positive or negative effect of formed nano and microstructures on osteogenic differentiation. For the UFG series, etched samples reach maximum ALP activity faster than the original polished titanium, but the higher ALP level was on the UFG-SP-15 sample, which did not had a developed surface topography and morphology. In terms of OPN expression, the difference between the samples of the UFG series is minimal. For the CG series, it is worth noting the relatively high values of ALP activity and OPN expression of the samples without developed morphology (CG-Ti and CG-SP-15).

In the general case, the results obtained by us correlate with the literature data. The difference in a number of in vitro tests between the results of this study and the literature data may be associated with differences in the topography, morphology, and composition of the surface of the samples, which occur with the smallest changes in the etching or the properties of the original titanium. For example, Zhang et al. found that there is a difference in surface morphology and in vitro results for rods and disks etched under the

same conditions, and the resulting micro/nanostructures are significantly better in ALP activity and OPN expression than micron/submicron structures [49].

5. Conclusions

1. Varying the etching duration and the type of etching solution (H_2SO_4/H_2O_2 or NH_4OH/H_2O_2) allows creating nano and microstructures of various morphology, topography, composition, and wettability on the surface of CG and UFG titanium. Etching of titanium in H_2SO_4/H_2O_2 leads to oxidation and an increase in the content of hydroxyl groups on the surface, which increases its hydrophilicity. Etching in NH_4OH/H_2O_2 does not lead to oxidation and reduces the amount of hydroxyl groups on the surface.

2. The conditions of chemical etching and the grain structure of the initial titanium have practically no effect on the viability and have no cytotoxic effect on MG-63 osteoblast-like cells.

3. UFG structure of titanium has a positive and decisive effect on the morphology and spreading of MG-63 cells. The cells on the etched UFG Ti have round shape, quickly form a monolayer and form cell strands, which indicates good and fast spreading and the potential for rapid proliferation and differentiation in the osteogenic direction.

4. Morphology and spreading MG-63 cells cultured for 24 h on samples of the CG series is worse than for the UFG series. However, these characteristics can be significantly improved by chemical etching and the creation of micro- and nanostructures on the surface.

5. UFG structure accelerates the proliferation of MG-63 cells at the later stages of the study (7 days); however, the factors of morphology, topography, and surface composition have a much greater influence.

6. Differentiation of MG-63 cells in the osteogenic direction is typical for all studied samples. The ALP activity dynamics of etched UFG titanium had a maximum, but for the CG series it does not appear. Nevertheless, the results of ALP activity and OPN expression studies have shown that the characteristics of differentiation are influenced by both grain structure and etching conditions.

Author Contributions: Conceptualization, D.N. and E.Z.; methodology, D.N., M.S. and E.Z.; validation, D.N. and V.S.; formal analysis, I.M. and D.N.; investigation, D.N., N.Y., M.S.; resources, E.Z. and M.M.; data curation, D.N. and M.M.; writing—original draft preparation, D.N., N.Y., I.M. and M.S.; writing—review and editing, D.N., E.Z., M.M., V.S. and M.S.; visualization, D.N. and I.M.; supervision, V.S.; project administration, E.Z., V.S. and D.N. All authors have read and agreed to the published version of the manuscript.

Institutional Review Board Statement: Not applicable.

Informed Consent Statement: Not applicable.

References

1. Geetha, M.; Singh, A.K.; Asokamani, R.; Gogia, A.K. Ti Based Biomaterials, the Ultimate Choice for Orthopaedic Implants-A review. *Prog. Mater. Sci.* **2009**, *54*, 397–425. [CrossRef]
2. Li, Y.; Yang, C.; Zhao, H.; Qu, S.; Li, X.; Li, Y. New Developments of Ti-Based Alloys for Biomedical Applications. *Materials* **2014**, *7*, 1709–1800. [CrossRef] [PubMed]
3. Brunette, D.M.; Tengvall, P.; Textor, M.; Thomsen, P. *Titanium in Medicine*; Springer: Berlin/Heidelberg, Germany; New York, NY, USA, 2001; pp. 1–1019.
4. Chen, Q.; Thouas, G.A. Metallic Implant Biomaterials. *Mater. Sci. Eng. R Rep.* **2015**, *87*, 1–57. [CrossRef]
5. Zhang, L.C.; Chen, L.Y. A Review on Biomedical Titanium Alloys: Recent Progress and Prospect. *Adv. Eng. Mater.* **2019**, *21*, 1801215. [CrossRef]
6. Matusiewicz, H. Potential Release of in vivo Trace Metals from Metallic Medical Implants in the Human Body: From Ions to Nanoparticles-A Systematic Analytical Review. *Acta Biomater.* **2014**, *10*, 2379–2403. [CrossRef] [PubMed]
7. Ortiz, A.J.; Fernandez, E.; Vicente, A.; Calvo, J.L.; Ortiz, C. Metallic Ions Released from Stainless Steel, Nickel-Free, and Titanium Orthodontic Alloys: Toxicity and DNA Damage. *Am. J. Orthod. Dentofac. Orthop.* **2011**, *140*, e115–e122. [CrossRef]
8. Valiev, R.Z.; Zhilyaev, A.P.; Langdon, T.G. *Bulk Nanostructured Materials: Fundamentals and Applications*; John Wiley &. Sons, Inc.: Hoboken, NJ, USA, 2014; pp. 1–440.
9. Mishnaevsky, L.; Levashov, E.; Valiev, R.Z.; Segurado, J.; Sabirov, I.; Enikeev, N.; Prokoshkin, S.; Solov'yov, A.V.; Korotitskiy, A.; Gutmanas, E.; et al. Nanostructured Titanium-Based Materials for Medical Implants: Modeling and Development. *Mater. Sci. Eng. R Rep.* **2014**, *81*, 1–19. [CrossRef]
10. Lowe, T.C.; Valiev, R.Z. Frontiers for Bulk Nanostructured Metals in Biomedical Applications. In *Advanced Biomaterials and Biodevices*; Tiwari, A., Nordin, A.N., Eds.; JohnWiley & Sons, Inc.: Hoboken, NJ, USA, 2014; pp. 1–52.
11. Semenova, I.P.; Polyakova, V.V.; Dyakonov, G.S.; Polyakov, A.V. Ultrafine-Grained Titanium-Based Alloys: Structure and Service Properties for Engineering Applications. *Advanced Engineering Materials* **2019**, *22*, 1900651. [CrossRef]
12. Bagherifard, S.; Ghelichi, R.; Khademhosseini, A.; Guagliano, M. Cell Response to Nanocrystallized Metallic Substrates Obtained Through Severe Plastic Deformation. *ACS Appl. Mater. Interfaces* **2014**, *6*, 7963–7985. [CrossRef]
13. Sotniczuk, A.; Garbacz, H. Nanostructured Bulk Titanium with Enhanced Properties—Strategies and Prospects for Dental Applications. *Adv. Eng. Mater.* **2021**, *202000909*, 1–19. [CrossRef]
14. Masrouri, M.; Faraji, G.; Pedram, M.S.; Sadrkhah, M. In-vivo Study of Ultrafine-Grained CP-Ti Dental Implants Surface Modified by SLActive with Excellent Wettability. *Int. J. Adhes. Adhes.* **2020**, *102*, 102684. [CrossRef]
15. Pippenger, B.E.; Rottmar, M.; Kopf, B.S.; Stubinger, S.; Dalla Torre, F.H.; Berner, S.; Maniura-Weber, K. Surface Modification of Ultrafine-Grained Titanium: Influence on Mechanical Properties, Cytocompatibility, and Osseointegration Potential. *Clin. Oral. Implant. Res.* **2019**, *30*, 99–110. [CrossRef]
16. Vetrone, F.; Variola, F.; De Oliveira, P.T.; Zalzal, S.F.; Yi, J.-H.; Sam, J.; Bombonato-Prado, K.F.; Sarkissian, A.; Perepichka, D.F.; Wuest, J.D.; et al. Nanoscale Oxidative Patterning of Metallic Surfaces to Modulate Cell Activity and Fate. *Nano Lett.* **2009**, *9*, 659–665. [CrossRef]
17. Variola, F.; Brunski, J.B.; Orsini, G.; Tambasco de Oliveira, P.; Wazen, R.; Nanci, A. Nanoscale Surface Modifications of Medically Relevant Metals: State-of-the Art and Perspectives. *Nanoscale* **2011**, *3*, 335–353. [CrossRef]
18. Richert, L.; Vetrone, F.; Yi, J.-H.; Zalzal, S.F.; Wuest, J.D.; Rosei, F.; Nanci, A. Surface Nanopatterning to Control Cell Growth. *Adv. Mater.* **2008**, *20*, 1488–1492. [CrossRef]
19. Nazarov, D.V.; Zemtsova, E.G.; Solokhin, A.Y.; Valiev, R.Z.; Smirnov, V.M. Modification of the Surface Topography and Composition of Ultrafine and Coarse Grained Titanium by Chemical Etching. *Nanomaterials* **2017**, *7*, 15. [CrossRef]
20. Nazarov, D.V.; Zemtsova, E.G.; Valiev, R.Z.; Smirnov, V.M. Formation of Micro- and Nanostructures on the Nanotitanium Surface by Chemical Etching and Deposition of Titania Films by Atomic Layer Deposition (ALD). *Materials* **2015**, *8*, 8366–8377. [CrossRef]
21. Moulder, J.F.; Stickle, W.F.; Sobol, P.E.; Bomben, K.D. *Handbook of X-ray Photoelectron Spectroscopy: A Reference Book of Standard Spectra for Identification and Interpretation of XPS Data*, 2nd ed.; Physical Electronics, Inc.: Eden Prairie, MN, USA, 1995; pp. 1–261.
22. Nazarov, D.V.; Smirnov, V.M.; Zemtsova, E.G.; Yudintceva, N.M.; Shevtsov, M.A.; Valiev, R.Z. Enhanced Osseointegrative Properties of Ultra-Fine-Grained Titanium Implants Modified by Chemical Etching and Atomic Layer Deposition. *ACS Biomater. Sci. Eng.* **2018**, *4*, 3268–3281. [CrossRef]

23. Chatakun, P.; Nunez-Toldra, R.; Diaz Lopez, E.J.; Gil-Recio, C.; Martinez-Sarra, E.; Hernandez-Alfaro, F.; Ferres-Padro, E.; Giner-Tarrida, L.; Atari, M. The Effect of Five Proteins on Stem Cells Used for Osteoblast Differentiation and Proliferation: A Current Review of the Literature. *Cell. Mol. Life Sci.* **2014**, *71*, 113–142. [CrossRef]

24. Zemtsova, E.G.; Yudintceva, N.M.; Morozov, P.E.; Valiev, R.Z.; Smirnov, V.M.; Shevtsov, M.A. Improved Osseointegration Properties of Hierarchical Microtopographic/Nanotopographic Coatings Fabricated on Titanium Implants. *Int. J. Nanomedicine* **2018**, *13*, 2175–2188. [CrossRef]

25. Medvedev, A.E.; Neumann, A.; Ng, H.P.; Lapovok, R.; Kasper, C.; Lowe, T.C.; Anumalasetty, V.N.; Estrin, Y. Combined Effect of Grain Refinement and Surface Modification of Pure Titanium on the Attachment of Mesenchymal Stem Cells and Osteoblast-Like SaOS-2 Cells. *Mater. Sci. Eng. C.* **2017**, *71*, 483–497. [CrossRef] [PubMed]

26. Biesinger, M.C.; Lau, L.W.M.; Gerson, A.R.; Smart, R.S.C. Resolving Surface Chemical States in XPS Analysis of First Row Transition Metals, Oxides and Hydroxides: Sc, Ti, V, Cu and Zn. *Appl. Surf. Sci.* **2010**, *257*, 887–898. [CrossRef]

27. Yi, J.-H.; Bernard, C.; Variola, F.; Zalzal, S.F.; Wuest, J.D.; Rosei, F.; Nanci, A. Characterization of a Bioactive Nanotextured Surface Created by Controlled Chemical Oxidation of Titanium. *Surf. Sci.* **2006**, *600*, 4613–4621. [CrossRef]

28. Lu, X.; Wang, Y.; Yang, X.; Zhang, Q.; Zhao, Z.; Weng, L.; Leng, Y. Spectroscopic Analysis of Titanium Surface Functional groups under Various Surface Modification and Their Behaviors In Vitro and In Vivo. *J. Biomed. Mater. Res. A* **2007**, *84*, 523–534. [CrossRef]

29. Kuznetsov, M.V.; Zhuravlev, J.F.; Zhilyaev, V.A.; Gubanov, V.A. XPS Study of the Nitrides, Oxides and Oxynitrides of Titanium. *J. Electron Spectrosc.* **1992**, *58*, 1–9. [CrossRef]

30. Martin, H.J.; Schulz, K.H.; Walters, K.B. Piranha Treated Titanium Compared to Passivated Titanium as Characterized by XPS. *Surf. Sci. Spectra* **2008**, *15*, 23–30. [CrossRef]

31. Lian, J.B.; Stein, G.S. Concepts of Osteoblast Growth and Differentiation: Basis for Modulation of Bone Cell Development and Tissue Formation. *Crit. Rev. Oral. Biol. Med.* **1992**, *3*, 269–305. [CrossRef]

32. Nie, F.L.; Zheng, Y.F.; Wei, S.C.; Wang, D.S.; Yu, Z.T.; Salimgareeva, G.K.; Polyakov, A.V.; Valiev, R.Z. In Vitro and In Vivo Studies on Nanocrystalline Ti Fabricated by Equal Channel Angular Pressing with Microcrystalline CP Ti as Control. *J. Biomed. Mater. Res. A* **2013**, *101*, 1694–1707. [CrossRef]

33. Zheng, C.Y.; Nie, F.L.; Zheng, Y.F.; Cheng, Y.; Wei, S.C.; Valiev, R.Z. Enhanced In Vitro Biocompatibility of Ultrafine-Grained Titanium with Hierarchical Porous Surface. *Appl. Surf. Sci.* **2011**, *257*, 5634–5640. [CrossRef]

34. Faghihi, S.; Azari, F.; Zhilyaev, A.P.; Szpunar, J.A.; Vali, H.; Tabrizian, M. Cellular and Molecular Interactions between MC3T3-E1 Pre-Osteoblasts and Nanostructured Titanium Produced by High-Pressure Torsion. *Biomaterials* **2007**, *28*, 3887–3895. [CrossRef]

35. Park, J.W.; Kim, Y.J.; Park, C.H.; Lee, D.H.; Ko, Y.G.; Jang, J.H.; Lee, C.S. Enhanced Osteoblast Response to an Equal Channel Angular Pressing-Processed Pure Titanium Substrate with Microrough Surface Topography. *Acta Biomater.* **2009**, *5*, 3272–3280. [CrossRef]

36. An, B.; Li, Z.; Diao, X.; Xin, H.; Zhang, Q.; Jia, X.; Wu, Y.; Li, K.; Guo, Y. In Vitro and In Vivo Studies of Ultrafine-Grain Ti as Dental Implant Material Processed by ECAP. *Mater. Sci. Eng. C Mater. Biol. Appl.* **2016**, *67*, 34–41. [CrossRef]

37. Estrin, Y.; Kasper, C.; Diederichs, S.; Lapovok, R. Accelerated Growth of Preosteoblastic Cells on Ultrafine Grained Titanium. *J. Biomed. Mater. Res. A* **2009**, *90*, 1239–1242. [CrossRef]

38. Lowe, T.C.; Reiss, R.A.; Illescas, P.E.; Davis, C.F.; Connick, M.C.; Sena, J.A. Effect of Surface Grain Boundary Density on Preosteoblast Proliferation on Titanium. *Mater. Res. Lett.* **2020**, *8*, 239–246. [CrossRef]

39. Zhao, M.; Wang, Q.; Lai, W.; Zhao, X.; Shen, H.; Nie, F.; Zheng, Y.; Wei, S.; Ji, J. In Vitro Bioactivity and Biocompatibility Evaluation of Bulk Nanostructured Titanium in Osteoblast-Like Cells by Quantitative Proteomic Analysis. *J. Mater. Chem. B* **2013**, *1*, 1926–1938. [CrossRef]

40. Hoseini, M.; Bocher, P.; Shahryari, A.; Azari, F.; Szpunar, J.A.; Vali, H. On the Importance of Crystallographic Texture in the Biocompatibility of Titanium Based Substrate. *J. Biomed. Mater. Res. A* **2014**, *102*, 3631–3638. [CrossRef]

41. Baek, S.M.; Shin, M.H.; Moon, J.; Jung, H.S.; Lee, S.A.; Hwang, W.; Yeom, J.T.; Hahn, S.K.; Kim, H.S. Superior Pre-Osteoblast Cell Response of Etched Ultrafine-Grained Titanium with a Controlled Crystallographic Orientation. *Sci. Rep.* **2017**, *7*, 44213. [CrossRef]

42. Kim, T.N.; Balakrishnan, A.; Lee, B.C.; Kim, W.S.; Smetana, K.; Park, J.K.; Panigrahi, B.B. In Vitro Biocompatibility of Equal Channel Angular Processed (ECAP) Titanium. *Biomed. Mater.* **2007**, *2*, S117–S120. [CrossRef]

43. Estrin, Y.; Ivanova, E.P.; Michalska, A.; Truong, V.K.; Lapovok, R.; Boyd, R. Accelerated Stem Cell Attachment to Ultrafine Grained Titanium. *Acta Biomater.* **2011**, *7*, 900–906. [CrossRef]

44. Lai, M.; Cai, K.; Hu, Y.; Yang, X.; Liu, Q. Regulation of the Behaviors of Mesenchymal Stem Cells by Surface Nanostructured Titanium. *Colloids Surf. B Biointerfaces* **2012**, *97*, 211–220. [CrossRef]

45. Bindu, S.; Sanosh, K.P.; Smetana, K.; Balakrishnan, A.; Kim, T.N. An In Vivo Evaluation of Ultra-Fine Grained Titanium Implants. *J. Mater. Sci. Technol.* **2009**, *25*, 556–560.

46. Attarilar, S.; Salehi, M.T.; Al-Fadhalah, K.J.; Djavanroodi, F.; Mozafari, M. Functionally Graded Titanium Implants: Characteristic Enhancement Induced by Combined Severe Plastic Deformation. *PLoS ONE* **2019**, *14*, e0221491. [CrossRef]

47. Kubacka, D.; Yamamoto, A.; Wieciński, P.; Garbacz, H. Biological Behavior of Titanium Processed by Severe Plastic Deformation. *Appl. Surf. Sci.* **2019**, *472*, 54–63. [CrossRef]

48. Kowalczyk-Gajewska, K.; Sztwiertnia, K.; Kawałko, J.; Wierzbanowski, K.; Wronski, M.; Frydrych, K.; Stupkiewicz, S.; Petryk, H. Texture Evolution in Titanium on Complex Deformation Paths: Experiment and Modelling. *Mater. Sci. Eng. A* **2015**, *637*, 251–263. [CrossRef]

49. Zhang, J.; Xi, Y.; Zuo, J.; Li, J.; Wei, Q.; Yu, Z.; Tang, Z. Cell Responses to Titanium Treated by a Sandblast-Free Method for Implant Applications. *Mater. Sci. Eng. C* **2017**, *78*, 1187–1194. [CrossRef]

50. Kang, Y.; Ren, X.; Yuan, X.; Ma, L.; Xie, Y.; Bian, Z.; Zuo, J.; Wang, X.; Yu, Z.; Zhou, K.; et al. The Effects of Combined Micron-scale Surface and Different Nanoscale Features on Cell Response. *Adv. Mater. Sci. Eng.* **2018**, *2018*, 1–9. [CrossRef]

51. Rosa, A.L.; Kato, R.B.; Castro Raucci, L.M.; Teixeira, L.N.; de Oliveira, F.S.; Bellesini, L.S.; de Oliveira, P.T.; Hassan, M.Q.; Beloti, M.M. Nanotopography Drives Stem Cell Fate Toward Osteoblast Differentiation Through Alpha1beta1 Integrin Signaling Pathway. *J. Cell. Biochem.* **2014**, *115*, 540–548. [CrossRef] [PubMed]

52. Souza, A.T.P.; Bezerra, B.L.S.; Oliveira, F.S.; Freitas, G.P.; Bighetti Trevisan, R.L.; Oliveira, P.T.; Rosa, A.L.; Beloti, M.M. Effect of Bone Morphogenetic Protein 9 on Osteoblast Differentiation of Cells Grown on Titanium with Nanotopography. *J. Cell. Biochem.* **2018**, *119*, 8441–8449. [CrossRef] [PubMed]

53. Kiran, A.S.K.; Sampath Kumar, T.S.; Perumal, G.; Sanghavi, R.; Doble, M.; Ramakrishna, S. Dual Nanofibrous Bioactive Coating and Antimicrobial Surface Treatment for Infection Resistant Titanium Implants. *Prog. Org. Coat.* **2018**, *121*, 112–119. [CrossRef]

54. Yuan, X.; Kang, Y.; Zuo, J.; Xie, Y.; Ma, L.; Ren, X.; Bian, Z.; Wei, Q.; Zhou, K.; Wang, X.; et al. Micro/Nano Hierarchical Structured Titanium Treated by NH_4OH/H_2O_2 for Enhancing Cell Response. *PLoS ONE* **2018**, *13*, e0196366. [CrossRef]

55. Sandeep Kranthi Kiran, A.; Sireesha, M.; Ramalingam, R.; Kizhakeyil, A.; Verma, N.K.; Lakshminarayanan, R.; Sampath Kumar, T.S.; Doble, M.; Ramakrishna, S. Modulation of Biological Properties by Grain Refinement and Surface Modification on Titanium Surfaces for Implant-Related Infections. *J. Mater. Sci.* **2019**, *54*, 13265–13282. [CrossRef]

56. Castro-Raucci, L.M.S.; Francischini, M.S.; Teixeira, L.N.; Ferraz, E.P.; Lopes, H.B.; de Oliveira, P.T.; Hassan, M.Q.; Rosa, A.L.; Beloti, M.M. Titanium With Nanotopography Induces Osteoblast Differentiation by Regulating Endogenous Bone Morphogenetic Protein Expression and Signaling Pathway. *J. Cell. Biochem.* **2016**, *117*, 1718–1726. [CrossRef]

57. Bello, G.D.; Fouillen, A.; Badia, A.; Nanci, A. A Nanoporous Titanium Surface Promotes the Maturation of Focal Adhesions and Formation of Filopodia with Distinctive Nanoscale Protrusions by Osteogenic Cells. *Acta Biomater.* **2017**, *60*, 339–349. [CrossRef]

58. Rodriguez-Contreras, A.; Bello, G.D.; Nanci, A. Surface Nanoporosity has a Greater Influence on Osteogenic and Bacterial Cell Adhesion than Crystallinity and Wettability. *Appl. Surf. Sci.* **2018**, *445*, 255–261. [CrossRef]

59. Arima, Y.; Iwata, H. Effect of Wettability and Surface Functional Groups on Protein Adsorption and Cell Adhesion using Well-Defined Mixed Self-Assembled Monolayers. *Biomaterials* **2007**, *28*, 3074–3082. [CrossRef]